

Theranostic Nanoplatfoms for PET Image-Guided Drug Delivery

Rubel Chakravarty, Feng Chen, Ashutosh Dash, and Weibo Cai

1 Introduction

Nanomedicine is often heralded as one of the major leaps forward for twenty-first century clinical practice [1–3]. The use of nanomaterials for cancer diagnosis and therapy is arguably the most active area of nanomedicine research. Despite extensive research input and huge investments, cancer remains a major public health concern worldwide [4]. Basically, this disease encompasses a heterogeneous spectrum of conditions and is highly unpredictable in majority of cases [4]. As per the statistics provided by World Health Organization (WHO), 8.2 million people worldwide died from cancer in 2012, out of which at least 30% of cancer deaths could have been prevented if necessary treatment was provided at an earlier time point [5]. Early diagnosis and treatment are essential to minimize the morbidity and mortality associated with the disease. In fact, early diagnosis of cancer is the crucial factor in majority of cases that directs the treatment regime and the choice of therapeutic intervention [4]. Successful cancer management relies on several factors that can be uniquely addressed via nanomedicine [1].

R. Chakravarty, Ph.D. (✉) • A. Dash
Isotope Production and Applications Division, Bhabha Atomic Research Centre,
Mumbai 400 085, India
e-mail: rubelc@barc.gov.in

F. Chen
Department of Radiology, University of Wisconsin, Madison, WI 53792-3252, USA

W. Cai, Ph.D. (✉)
Department of Radiology, University of Wisconsin, Madison, WI 53792-3252, USA
Department of Medical Physics, University of Wisconsin, Madison, WI 53705-2275, USA
Carbone Cancer Center, University of Wisconsin, Madison, WI 53792-3252, USA
e-mail: wcai@uwhealth.org

Conventional cancer treatment approaches rely on systemic administration of chemotherapeutic drugs that indiscriminately affect tumor and healthy tissue alike, and therefore are toxic to both types of tissues [6, 7]. Such strategies are limited by a narrow therapeutic index (ratio of therapeutic to toxic effects) and demonstrate severe systemic side effects [8]. Additionally, several routinely used chemotherapeutic drugs suffer from poor pharmacokinetics and inappropriate biodistribution that greatly limits the maximum allowable dose of the drug [3, 6, 8]. Therefore, many conventional drugs that have been shown to be highly effective *in vitro* are often relatively ineffective when administered *in vivo*. From this perspective, the use of nanoplatforms for targeted drug delivery can increase the selectivity of the treatment, improve drug concentration at the tumor site, and maximize the therapeutic response while minimizing toxic side effects [3, 7, 9].

The past 10 years have witnessed significant advances in the development and deployment of nanoplatforms for targeted drug delivery, and innovative applications of cancer nanomedicine are now coming to fruition [3, 6–10]. Numerous nanoparticle-based products for drug delivery have been approved for clinical applications, and even more are currently in clinical trials [3, 7]. An important breakthrough in this direction is the development of multifunctional nanoplatforms—nanoparticles that are capable of accomplishing multiple objectives such as imaging and targeted therapy or performing a single advanced function through incorporation of multiple functional units [10–12]. The synergistic utilization of a single nanoplatform for both molecular imaging as well as targeted drug delivery is known as “image-guided drug delivery,” which is a promising attribute toward personalized cancer management [9, 11, 12].

By adopting molecular imaging approaches it is possible to noninvasively visualize how well these nanoplatforms can accumulate at the target site and specifically deliver the drug molecules [11]. It is also possible to preselect patients who are likely to respond to such treatment procedures. This strategy also offers a way to monitor how well patients would respond to nanomedicine-based therapeutic interventions, based on which drug doses and treatment protocols can be individualized and optimized during follow-up. Molecular imaging information on the possible accumulation of nanomedicine formulations in endangered healthy tissues may be used to exclude patients from further treatment.

The field of image-guided drug delivery has witnessed rapid advancement over the last few years which could be attributed to the phenomenal growth of molecular imaging technologies [11–13]. Various imaging modalities [e.g., positron emission tomography (PET), single photon emission computed tomography (SPECT), magnetic resonance imaging (MRI), optical, ultrasound] are now routinely used to assess specific molecular targets in preclinical and clinical settings [13–15]. Among these molecular imaging modalities, PET imaging is becoming more prevalent in clinical practices all over the world particularly because of its high sensitivity and possibility for accurate quantification which helps in understanding biological processes at the molecular and metabolic levels *in vivo* [16]. Despite excellent attributes of PET technology in the field of clinical molecular imaging, it must be stressed here that no single imaging modality can provide information on all aspects of structure and function [17]. The choice of a particular imaging modality is primarily dependent on the specific question to be addressed through molecular imaging approach.

This chapter focuses on the inherent feasibility and practicality of the concept of PET image-guided drug delivery using nanoplatfoms. The development of theranostic nanoplatfoms for site- and event-specific targeting and controlled drug release are summarized, and the great potential and fascinating prospects for forthcoming developments that might help in translating the research results from “bench-to bedside” are discussed.

2 PET Imaging as a Tool to Guide Drug Delivery

PET is a sensitive and specific noninvasive imaging modality that employs external detectors to measure the three dimensional distribution and pharmacokinetics of injected drug-loaded nanoplatfoms that have been radiolabeled with suitable positron emitting radioisotopes [16, 18]. After being emitted from the nucleus, the positron travels a short distance in the surrounding matter or tissue before it annihilates with an electron to produce two 511 keV γ -rays, which correspond to the rest masses of the positron and electron [16]. These γ -rays are emitted simultaneously in opposite directions and are then detected by an array of surrounding detectors connected in coincidence mode. Generally, a large number of coincidence events are acquired within a very narrow time interval (nanoseconds). The data is stored in the form two-dimensional matrices called sonograms that are then corrected for detector nonuniformity of response, attenuation of photons by body and scatter, and reconstructed into an image with information on the spatial distribution of radioactivity as a function of time.

The ability to measure pharmacokinetics of drug-loaded nanoplatfoms in tissues with PET needs to be underpinned by strong radiochemistry input [16, 18]. Several positron-emitting radioisotopes can be used to radiolabel drug-loaded nanoplatfoms for research and clinical use, summary of which along with their nuclear decay properties is provided in Table 1. The availability of a wide variety of radioisotopes makes it possible to carefully pick the specific nuclear properties that are needed for a particular application in PET image-guided drug delivery [16]. From the perspective of PET imaging, ^{18}F ($t_{1/2}=110$ min) and ^{68}Ga ($t_{1/2}=68$ min) appear to be ideal choices because of their almost perfect chemical and nuclear decay characteristics. Indeed, these two radioisotopes are most widely used for preparing conventional PET radiopharmaceuticals for routine clinical use all over the world [19, 20]. However, ^{18}F and ^{68}Ga may not be suitable for use in PET image-guided drug delivery as their short decay half-lives do not match the pharmacokinetics of most drug-loaded nanoplatfoms. Moreover, the radiolabeling step might be time consuming, especially, in case of chelator-free radiolabeling of nanoplatfoms [21–23], wherein use of these short-lived radioisotopes might not be economically viable. From this perspective, the use of nonconventional radioisotopes such as ^{44}Sc , ^{64}Cu , ^{69}Ge , ^{86}Y , ^{89}Zr , etc. (Table 1), with relatively longer half-lives, might be beneficial [24, 25]. However, it is pertinent to point out that most of these radioisotopes emit high energy γ -photons (with relatively high abundance) caused by a complex decay scheme. These γ -photons can be detected in addition to the coincidence photons resulting from the positron emission, thereby increasing the spurious event rate, which leads to inferior imaging quality and

Table 1 Nuclear decay characteristics of some positron emitting radioisotopes that can be used for PET image-guided drug delivery

Radionuclide	Half-life (h)	Mode of decay	β^+ Particle energy (MeV) ^{a,b}	β^+ - Branching ratio (%) ^b	Major γ -photons emitted other than annihilation photons in MeV (% abundance)
¹⁸ F	1.8	β^+ /ECD	0.633	97.0	None
⁴⁴ Sc	3.9	β^+ /ECD	1.474	94.3	1.157 (99.9)
⁶⁴ Cu	12.7	β^+ / β^- /ECD	0.653	17.4	1.346 (0.47)
⁶⁸ Ga	1.1	β^+ /ECD	1.889	88.0	1.077 (3.3)
⁶⁹ Ge	39.1	β^+ /ECD	1.205	21.0	0.574 (13.3), 0.872 (11.9)
⁷² As	26.0	β^+ /ECD	2.499	64.2	0.630 (7.9), 0.834 (80.0),
⁸⁶ Y	14.7	β^+ /ECD	1.220	11.9	0.443 (16.9), 0.646 (9.2), 0.777 (22.4), 1.854 (17.4), 1.920 (20.8)
⁸⁹ Zr	78.4	β^+ /ECD	0.897	23.0	0.909 (100)

ECD electron capture decay

^aMaximum β^+ energy is mentioned

^bOnly principal β^+ emission is indicated

degradation of the quantitative accuracy. Therefore, depending on the specific application, a balance between half-life of the radioisotope and the image quality which is dependent on nuclear decay characteristics of the radioisotope needs to be considered for choosing the appropriate radioisotope for labeling the desired nanoplatform.

PET images acquired after in vivo administration of radiolabeled nanoplatforms are generally analyzed by defining regions of interest and extracting radioactivity versus time-curves for the region [16, 18]. In more realistic circumstances, functional parametric images are generated on a voxel-to-voxel basis using generic kinetic analysis [18]. If effect of drug-loaded nanoplatforms needs to be quantified, mathematical kinetic modeling approach can be employed [16, 18]. This strategy helps to enhance data interpretation within a framework of important kinetic behavior in the region of interest to obtain quantitative parameters of relevance and universal comprehension. Mathematical modeling of PET data also enables pharmacological and physiological parameters that can be used to quantitatively assess the in vivo behavior of drug-loaded nanoplatforms [16, 18].

3 Radiolabeled Nanoplatforms for PET Image-Guided Drug Delivery

In order to achieve image-guided drug delivery, researchers have developed several nanoplatforms with diverse sizes, architectures, and surface properties for selective administration of the chemotherapeutic drug to a specific target location [11, 12]. Some typical examples of nanoplatforms that have been particularly found to be useful for PET-image-guided drug delivery include organic nanoparticles such as

liposomes, micelles, endogenous nanostructures, and inorganic nanoparticles such as colloidal metals and oxide nanoparticles [11, 26]. For a particular application, the choice of the nanoplatfom is influenced by the bioavailability, biodistribution, types of drugs that can be delivered, and the specificity and pharmacokinetics of delivery. The *in vivo* stability and fate of the drug-loaded nanoplatfoms is decided by numerous factors such as size, rigidity, charge, solubility, and surface modifications of the nanoplatfom. With the advances in material science and nanotechnology, it is now possible to specifically tailor these properties during the synthesis of nanoplatfoms for targeted delivery of requisite doses of chemotherapeutic drugs and imaging contrast agents into cancerous lesions while sparing the healthy tissues. Such “smart” theranostic nanoplatfoms hold out the possibility of radically changing the practice of cancer management, allowing easy diagnosis followed by effective targeted therapy at the early stages of the disease.

Generally, two strategies are used for loading drugs onto targeting nanoplatfoms [11, 12]. In the first approach, drugs are directly conjugated to the nanoplatfoms surface using suitable linkers [11, 12]. The major limitations of this approach include (a) potential alteration in property of the drug due to conjugation, (b) inevitable heterogeneity of the final product, and (c) the need to develop customized conjugation procedure for each particular drug that needs to be delivered using the nanoplatfom [11, 12]. Many of these limitations could be circumvented to a considerable extent in the other approach, which involves loading of chemotherapeutic drugs onto high capacity nanoplatfoms (e.g., liposomes, inorganic oxides, etc.) [11, 12]. Such drug-loaded nanoplatfoms protect entrapped drugs from degradation during their delivery to the target and do not alter the biological efficacy of the drug [11, 12]. Despite excellent attributes of this strategy for PET image-guided drug delivery, drug release from the nanoplatfoms cannot always be properly triggered to take place with the desired selectivity [27]. Moreover, homogeneous distribution and effective internalization of the drugs by the whole population of targeted cancerous cells are not always achievable [27]. Nevertheless, it would be possible to achieve sustained drug release over a prolonged period of time by modulating the porosity, surface charge, and biodegradability of the nanoplatfoms.

The delivery of the nanoplatfom to the target tissue can be achieved primarily in two ways—passive and active targeting (Fig. 1) [28]. Passive targeting takes advantage of the permeability of tumor tissue [28]. Due to rapid vascularization to serve fast-growing cancerous tissues, the capillary endothelium in cancerous tissue is more disorderly and thus more permeable toward nanoplatfoms than the capillary endothelium in normal tissues. If the drug-loaded nanoplatfom can stay in blood circulation for a reasonably long time, there will be enrichment of nanoplatfoms into the tumor tissues. Furthermore, since the lymphatic system is not developed in tumor tissue, extravasated nanoparticles tend to stay inside the interstitial space in tumor tissues. This overall phenomenon of accumulation of nanoplatfoms in tumor tissues is known as the enhanced permeability and retention (EPR) effect [28].

The EPR phenomenon is dependent on several factors such as particle size, particle surface charge and hydrophobicity, immunogenicity, tumor characteristics, etc., which results in many challenges in the optimization of passive targeting [28].

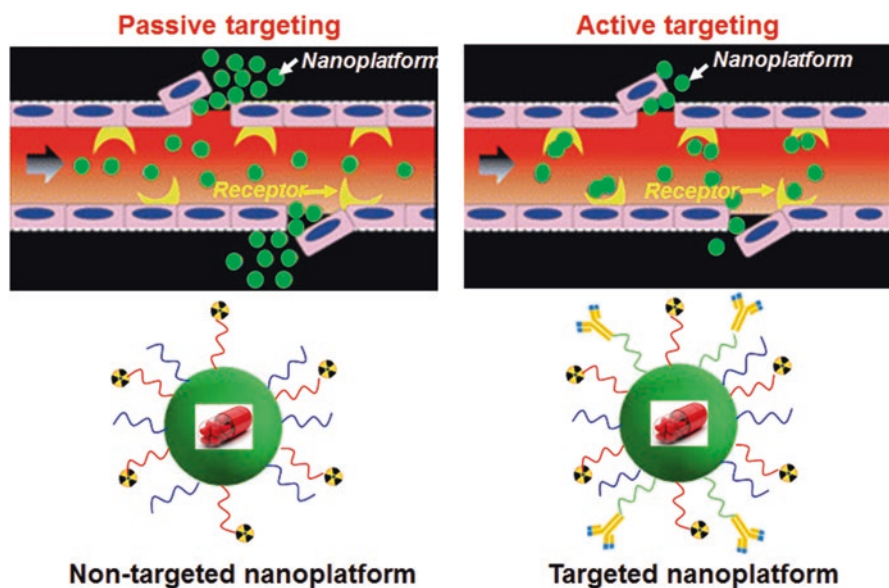


Fig. 1 Schematic depiction of EPR-mediated passive and active targeting using theranostic nanoplateforms. Nanoparticles can passively target tumors through preferential passage through larger interendothelial junctions compared to those of healthy tissues. Nanoparticles can also be conjugated with suitable targeting agents, such as antibodies that are specific to proteins (receptors) more highly expressed in tumors than healthy tissue, to actively target tumors. Adapted with permission from Ref. [28]

Further, specificity toward the tumor would be low in passive targeting and therefore therapeutic concentrations of the chemotherapeutic drug can be suboptimal at the tumor site resulting in poor therapeutic efficacy [11]. To overcome these limitations, active targeting would be a more viable approach that can be achieved by conjugating the functionalized nanoplateform to a suitable targeting moiety such as aptamers, peptides, or proteins, thereby allowing preferential accumulation of the drug in the tumor tissue [28]. The best results would be expected by combining the effects of both passive and active targeting to achieve maximal therapeutic efficacy [11].

A major hurdle in using nanoplateforms for image-guided drug delivery is their tendency to get trapped and cleared from the circulation by the reticuloendothelial system (RES) [27]. Additionally, nanoparticles can interact with plasma proteins effectively altering their surface properties [27]. The introduction of biocompatible hydrophilic polymer chains, such as polyethylene glycol (PEG), creates a hydrated brush-like coating on the nanoparticle surface that enhances nanoparticle solubility, prolongs blood circulation times, and delays RES clearance [29, 30]. It has been demonstrated that PEG-coated nanoplateforms have circulation times several orders of magnitude longer than uncoated nanoplateforms [29, 30]. Various nanoplateforms have been radiolabeled with different positron emitting radioisotopes for PET image-guided drug delivery, most of which are summarized in Table 2 and discussed in the following text.

Table 2 Representative examples of theranostic nanoplatforms utilized for PET image-guided drug delivery

Drug carrier	Targeting ligand	Target	Therapeutic agent	PET isotope	Disease model	Tumor uptake	References
Liposome	None (passive targeting)	None (passive targeting)	Model hydrophilic drug	^{18}F and ^{64}Cu	Met-1 tumors	(Not reported)	[33]
Micelles	cRGD peptide	Integrin $\alpha_v\beta_3$	Doxorubicin	^{64}Cu	Human glioblastoma	~7% ID/g	[37]
Melamin nanoparticles	None (passive targeting)	None (passive targeting)	Sorafenib	^{64}Cu	Hepatocellular carcinoma	~5.5% ID/g	[26]
Gold nanorods	cRGD peptide	Integrin $\alpha_v\beta_3$	Doxorubicin	^{64}Cu	Human glioblastoma	~6% ID/g	[44]
Mesoporous silica nanoparticles	TRC105 antibody	CD105	Doxorubicin	^{64}Cu	Murine breast cancer	~6% ID/g	[49]

3.1 *Liposomes for PET Image-Guided Drug Delivery*

Liposomes are good candidates as drug carriers and have been widely investigated in drug delivery systems [31, 32]. Basically, liposomes are self-assembled vesicles composed of a lipid bilayer, which forms a closed shell surrounding an internal aqueous phase. The major advantages of liposomal carriers for drug delivery are that they are biodegradable and nontoxic [31, 32]. Moreover, size, charge, and surface functionalization of liposomes are easily controllable and such systems are suitable for carrying both hydrophobic and hydrophilic drug molecules [31, 32]. Owing to these favorable characteristics, liposomes were the first nanoplateforms to make the transition from conceptual stage to clinical application, and are now an established technology platform with considerable clinical acceptance [7, 31, 32].

Paoli et al. reported the synthesis of liposomal formulations with particle size in the range 80–113 nm [33]. The liposomes were pre-conjugated with suitable fluorophores (calcein or AF-750) and radiolabeled with ^{18}F or ^{64}Cu for dual-modality PET/optical imaging. A model hydrophilic drug was encapsulated in the liposomal system and administered in mice bearing bilateral Met-1 tumors, to assess the relative stability and circulation kinetics of the drug-loaded liposomes, while maintaining temperature sensitivity. Using *in vivo* PET imaging and *ex vivo* fluorescent imaging of tumors, the authors could demonstrate that the accumulation of the drug was increased by up to 177-fold by liposomal encapsulation.

In a recent study, Lee et al. reported the synthesis of a chelator compound, 4-DEAP-ATSC, which serves as the ^{64}Cu loading and entrapment agent in liposomal formulations [34]. The authors demonstrated that the ^{64}Cu -DEAP-ATSC complex could be loaded into PEGylated liposomal doxorubicin (PLD) and HER2-targeted PLD (MM-302) with >90% efficiency and that ^{64}Cu -loaded liposomal formulations were stable in human plasma up to 24 h. *In vivo* PET imaging studies in BT474-M3 (HER2-overexpressing breast carcinoma) xenografts after administration of ^{64}Cu -MM-302 showed heterogeneous distribution within tumors. The biodistribution profiles were quantitatively consistent with tissue-based analysis, and radioactivity uptake in the tumor (4.8 ± 0.7 %ID/g at 24 h postinjection) correlated with liposomal drug deposition. The promising results obtained in this study suggest that clinical translation of this strategy might aid in the identification of cancer patients who are most suited for undergoing liposomal therapy.

3.2 *Micelles for PET Image-Guided Drug Delivery*

Micelles are colloidal particles with a size usually within a range of 5–100 nm, and are currently under investigation for targeted delivery of hydrophobic anticancer drugs [35]. When tagged with suitable positron emitting radioisotopes, these systems can be used for image-guided drug delivery. Among the various micellar structures, the polymeric micelles are the most extensively used for drug delivery applications [35, 36]. The polymeric micelles generally consist of a unique core–shell structure.

The inner core is the hydrophobic part of the block copolymer, which encapsulates the hydrophobic drug. The outer shell or corona of the hydrophilic block of the copolymer is often composed of PEG, and it protects the drug from the aqueous environment and also imparts particle stability and excellent dispersibility in an aqueous solution. Because of these characteristics, polymeric micelles have several advantages as drug carriers such as enhancing the aqueous solubility of hydrophobic drugs, prolonging the circulation time of the drug in the blood, improving the in vivo stability of the drug, providing both passive and active tumor targeting abilities, and reducing nonspecific uptake by the RES [35, 36].

In the first use of micellar systems for PET image-guided drug delivery in tumor-bearing mice, Xiao et al. reported the synthesis of multifunctional unimolecular micelles made of a hyperbranched amphiphilic block copolymer [37]. The hyperbranched block copolymer of the micellar system was conjugated with cyclo(Arg-Gly-Asp-D-Phe-Cys) peptides (cRGD, for integrins $\alpha_v\beta_3$ targeting) and macrocyclic chelators [1,4,7-triazacyclononane-*N,N,N'*-triacetic acid (NOTA)], for ^{64}Cu -labeling. An anticancer drug, doxorubicin (DOX), was also covalently conjugated onto the hydrophobic segments of the amphiphilic block copolymer arm to enable targeted drug delivery and pH-controlled drug release. In vitro studies showed that cRGD-conjugated unimolecular micelles exhibited a much higher cellular uptake in human glioblastoma (U87MG) cells due to integrin $\alpha_v\beta_3$ -mediated endocytosis compared to nontargeted unimolecular micelles, thereby leading to a significantly higher cytotoxicity. In vivo PET imaging and biodistribution studies in U87MG (human glioblastoma) xenografts revealed that targeted unimolecular micelles (conjugated with cRGD peptide) exhibited a much higher level of tumor accumulation ($\sim 5\%$ ID/g) than nontargeted unimolecular micelles ($\sim 2.5\%$ ID/g) at 4 h postinjection (Fig. 2a). Administration of a blocking dose of cRGD peptide (10 mg/kg of mouse body weight) followed by administration of radiolabeled unimolecular micelle conjugated with cRGD peptide reduced the tumor uptake significantly ($\sim 2\%$ ID/g), which confirmed integrin $\alpha_v\beta_3$ specificity of the targeted micelle in vivo (Fig. 2a). These results were further confirmed by ex vivo optical imaging using the fluorescence signal of DOX (Fig. 2b).

The same group of authors further extended the work by conjugation of anti-CD105 monoclonal antibody (TRC105) with the unimolecular micelles (instead of cRGD peptide as done in the previous study) [38]. TRC105-conjugated unimolecular micelles showed a higher CD105-associated cellular uptake in human umbilical vein endothelial cells (HUVEC) compared with nontargeted unimolecular micelles. Similar to the previous study, in vivo PET imaging and biodistribution studies in 4T1 murine breast tumor-bearing mice showed that a tumor accumulation of $\sim 6\%$ ID/g of targeted micelles (i.e., conjugated with TRC105) was higher than that of nontargeted micelles ($\sim 3\%$ ID/g) at 5 h postinjection. In a recent study, the same group of authors reported the development of a new type of unimolecular micelle formed by brush-shaped amphiphilic block copolymers [39]. As in the previous study, the unimolecular micelle was conjugated with TRC105, loaded with DOX and radiolabeled with ^{64}Cu for PET image-guided drug delivery in 4T1 tumor-bearing mice and similar results were obtained. The encouraging results obtained in all these studies clearly indicate that unimolecular micelles are promising form of nanomedicine for targeted cancer theranostics.

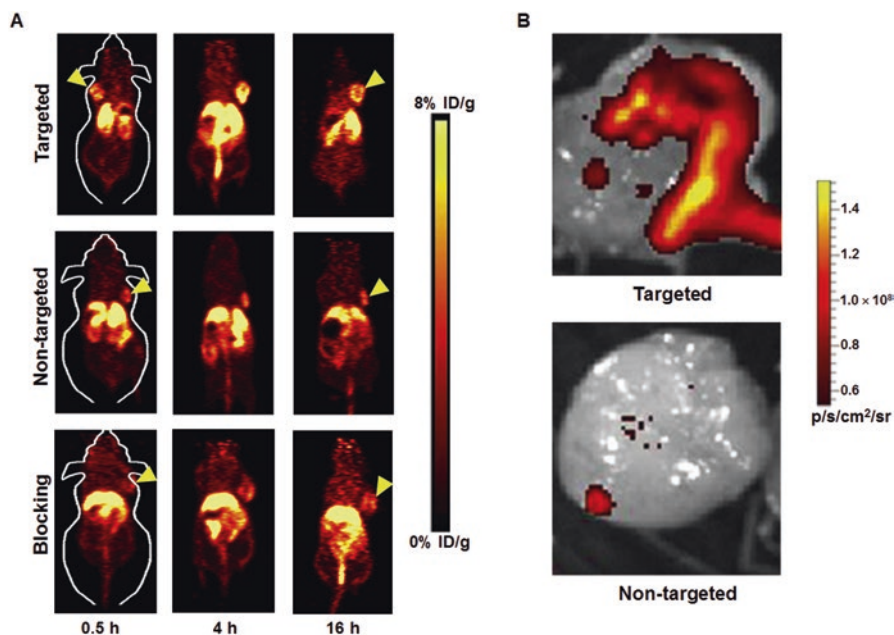


Fig. 2 PET image-guided drug delivery using unimolecular micelle. (a) PET imaging of U87MG tumor-bearing mice at different time points postinjection of ^{64}Cu -labeled unimolecular micelle loaded with DOX (nontargeted), ^{64}Cu -labeled unimolecular micelle conjugated to cRGD and loaded with DOX (targeted), and ^{64}Cu -labeled unimolecular micelle conjugated to cRGD and loaded with DOX with a blocking dose of cRGD (blocking). (b) Ex vivo fluorescence imaging of U87MG tumor, with the excitation and emission set for detecting DOX fluorescence, harvested from mice injected with targeted and nontargeted unimolecular micelles. Adapted with permission from Ref. [37]

3.3 Endogenous Nanosystems for PET Image-guided Drug Delivery

Over the last few years, there is growing interest toward the use of endogenous organic nanostructures, such as ferritins, melanin, etc. as drug delivery platforms due to their native biocompatibility and biodegradability [26, 40, 41]. In this direction, it is desirable to develop endogenous systems that intrinsically possess both contrast and drug delivery properties. Recently, Zhang et al. reported the synthesis of melanin nanoparticles as an efficient endogenous system for multimodality image-guided drug delivery [26]. Melanin is a biopolymer with good biocompatibility and biodegradability, intrinsic photoacoustic properties, and binding ability to various types of chemotherapeutic drugs [41]. The synthesized nanoparticles were PEGylated, loaded with an anticancer drug (Sorafenib), radiolabeled with a ^{64}Cu adopting chelator-free approach, and then used for dual modality PET and photoacoustic image-guided drug delivery. In vivo PET imaging and biodistribution studies after intravenous administration of the nanoplatforms in hepatocellular carcinoma

(HepG2) tumor-bearing mice revealed rapid tumor uptake by passive targeting (5.5 ± 0.3 % ID/g at 4 h postinjection) with a good tumor to background contrast. The results of PET imaging were further corroborated by photoacoustic imaging. Furthermore, the authors could successfully demonstrate the antitumor effects of drug-loaded melanin nanoparticles by studying the inhibition of tumor growth in vivo. The promising results obtained in this study prove that melanin nanoparticles are an efficient biosystem for multimodality image-guided drug delivery and hold potential for clinical translation in the foreseeable future.

3.4 Metallic Nanoparticles for PET Image-Guided Drug Delivery

Among the various metallic nanoparticles reported to date, gold nanostructures possess unique characteristics that enable their use as contrast agents, therapeutic entities, and frameworks to attach functional molecules, therapeutic cargo, or targeting ligands [42, 43]. Owing to their ease of synthesis, easy surface functionalization, and nontoxicity, gold nanostructures have emerged as powerful nanoplatforms for cancer theranostics [42]. The development of a multifunctional gold nanorod-based nanoplatfor for PET image-guided drug delivery was reported by Xiao et al. [44]. The bare gold nanorods had a length and diameter of approximately 45 and 10 nm, respectively. The gold nanorods were PEGylated and an anticancer drug (DOX) and tumor targeting agent (cRGD) were conjugated to it. A chelator, NOTA, was attached onto the distal ends of the PEG arms for ^{64}Cu labeling. Based on flow cytometry analysis, cRGD-conjugated gold nanorods loaded with DOX exhibited a higher uptake and cytotoxicity in U87MG cells compared to nontargeted gold nanorods in vitro. However, in vivo PET imaging and biodistribution studies showed that targeted and nontargeted gold nanorods had a similar distribution pattern, in particular in respect to tumor uptake (~ 5 % ID/g). Despite this limitation, this study demonstrated the potential of gold nanorods as an efficient nanoplatfor for cancer theranostics.

3.5 Inorganic Oxide Nanoparticles for PET Image-Guided Drug Delivery

Over the last few years, inorganic oxide nanoparticles such as silica and iron oxide nanoparticles have gained significant attention for image-guided drug delivery due to their easy synthesis, uniform morphology, adjustable pore volume, controllable diameter, modifiable surface potential, possibility for easy functionalization, and significant biocompatibility [45–47]. Owing to these favorable features, dye-doped ultrasmall and renal clearable silica nanoparticles (also known as C dots) have recently received the United States Food and Drug Administration (FDA) investigational new drug approval for a first-in-man clinical trial [48].

The utilization of silica nanoparticles for PET image-guided drug delivery in small animal models was reported by Chen et al. [49]. The authors synthesized uniform 80 nm sized mesoporous silica nanoparticles (MSNs), which were then surface functionalized with thiol groups, PEGylated, conjugated with NOTA chelator and TRC105 antibody (specific for CD105/endoglin). The nanoplatform was loaded with an anticancer drug, DOX, and radiolabeled with ^{64}Cu for PET image-guided drug delivery in 4T1 murine breast tumor-bearing mice. In vivo PET imaging and biodistribution studies showed high tumor uptake ($\sim 6\%$ ID/g) at 5 h postinjection. The tumor uptake ($\sim 3\%$ ID/g at 5 h postinjection) of nontargeted nanoparticles (not conjugated with TRC105) was lower than the tumor uptake observed with targeted nanoparticles, indicating that both active targeting and EPR effect were responsible for the enhanced tumor uptake. The CD105 specificity of the TRC105-conjugated nanoplatform was further confirmed by blocking studies, wherein administration of a blocking dose (1 mg/mouse) of TRC105 at 1 h before injection of radiolabeled nanoplatform could significantly reduce the tumor uptake to $\sim 3\%$ ID/g at 5 h postinjection. The loading capacity of DOX in MSNs was estimated to range from 76.6 to 481.6 mg/g. Using ex vivo optical imaging, the authors could successfully demonstrate the feasibility of enhanced tumor targeted delivery of DOX using TRC105-conjugated MSNs. In another similar study from the same group, MSNs were PEGylated, conjugated with anti-vascular endothelial growth factor receptor (VEGFR) ligand, VEGF₁₂₁, loaded with anti-VEGFR drug (sunitinib), and radiolabeled with ^{64}Cu for PET image-guided drug delivery in human glioblastoma (U87MG) xenografts [50]. As observed in the previous study, significantly higher amount of drug could be delivered to the tumor by targeting VEGFR when compared with the nontargeted counterparts.

In order to achieve a higher drug loading capacity and improved tumor uptake than MSNs, Chen et al. reported the synthesis of functionalized hollow mesoporous silica nanoparticles (HMSNs) of 150 nm particle size [51]. The drug (DOX) loading capacity of HMSNs was found to be 3–15 times higher than previously reported MSNs [49, 51]. The hollow space inside the nanoplatform could be loaded with DOX, followed by conjugation with near-infrared (NIR) dye (ZW800) and the ^{64}Cu -chelator NOTA. The drug-loaded nanoplatform was subsequently PEGylated, conjugated with TRC105 antibody, and radiolabeled with ^{64}Cu for dual modality (PET/optical) image-guided drug delivery in 4T1 tumor-bearing mice. In vivo PET imaging and biodistribution studies revealed that tumor uptake of TRC105-conjugated HMSNs was $\sim 10\%$ ID/g at 4 h postinjection, which was ~ 3 times higher than that of the nontargeted group (Fig. 3a). Administration of a blocking dose (1 mg/mouse) of free TRC105 at 1 h before injection of radiolabeled nanoplatform could significantly reduce the tumor uptake to $\sim 5\%$ ID/g at 4 h postinjection, clearly demonstrating CD105 specificity of the targeted nanoplatform in vivo (Fig. 3a). These results were further corroborated by optical imaging studies. Enhanced DOX delivery was also demonstrated in 4T1 tumor-bearing mice by ex vivo optical imaging using fluorescence signal of DOX (Fig. 3b). This work was further extended by the same group, wherein ^{64}Cu -labeled HMSNs were loaded with anticancer drug (sunitinib), and conjugated with cRGD peptide for targeting integrin $\alpha_v\beta_3$ expression in U87MG tumor-bearing mice [52]. In vivo PET imaging studies indicated $\sim 8\%$ ID/g tumor uptake of targeted nanoconju-

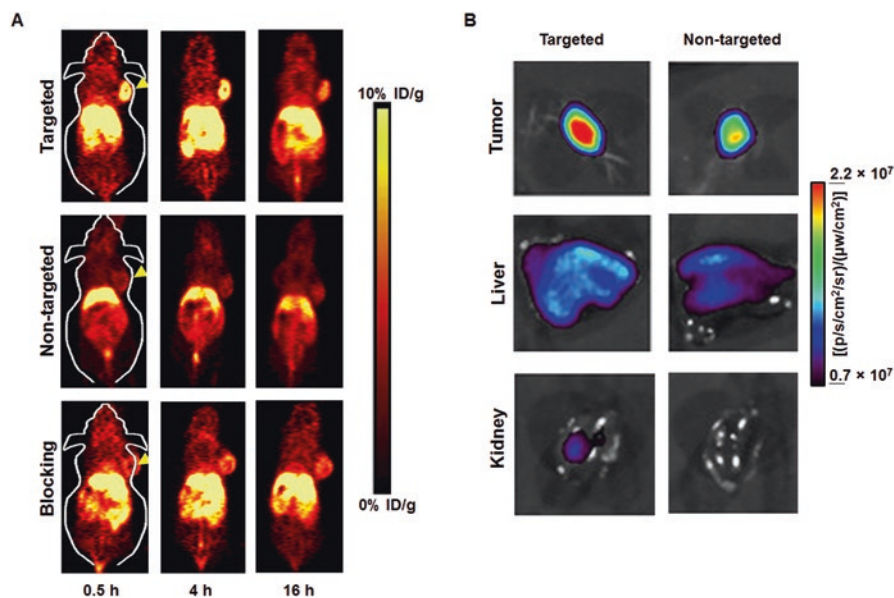


Fig. 3 PET image-guided drug delivery using HMSNs. (a) PET images of 4T1 tumor-bearing mice at different time points postinjection of ^{64}Cu -labeled HMSNs loaded with DOX (nontargeted), ^{64}Cu -labeled HMSNs conjugated to TRC105 and loaded with DOX (targeted), and ^{64}Cu -labeled HMSNs conjugated to TRC105 and loaded with DOX with a blocking dose of TRC105 (blocking). (b) Ex vivo optical imaging of major organs in 4T1 tumor-bearing mice with the excitation and emission set for detecting DOX fluorescence after intravenous injection of targeted and nontargeted HMSNs. Adapted with permission from Ref. [51]

gates, which correlated well with ex vivo biodistribution analyses. As in the previous study, enhanced tumor-targeted delivery of the anticancer drug was observed, thereby demonstrating the potential of HMSNs for targeted cancer imaging and drug delivery. Since silica-based nanoparticles have already received FDA approval for clinical use [48], the results obtained in these studies set the stage toward potential clinical translational of this promising nanoplatform for cancer theranostics.

Iron oxide nanoparticles are used as contrast agents in magnetic resonance imaging (MRI) [46, 47]. Additionally, such nanoparticles offer the scope of attaching probes containing multiple imaging motifs on its surface for multimodality molecular image-guided drug delivery [46, 47]. In an interesting study, Yang et al. reported the synthesis of cRGD-functionalized, DOX-conjugated, and ^{64}Cu -labeled superparamagnetic iron oxide nanoparticles (SPIOs) for targeted anticancer drug delivery and PET/MR imaging in human glioblastoma (U87MG) xenografts [53]. In vivo PET imaging and biodistribution studies showed that cRGD-conjugated SPIOs showed a much higher level of tumor accumulation ($\sim 5\%$ ID/g) than nontargeted, i.e., cRGD-free ones ($< 2\%$ ID/g). From relaxivity measurements, it was demonstrated that drug-loaded and cRGD-conjugated SPION could effectively serve as MR contrast agents. The authors also observed that cRGD-conjugated SPIOs induced a significant amount of cytotoxicity in the U87MG tumor cells, suggesting that DOX was released from

the nanoplatform and entered the cell nucleus. This study successfully demonstrates the potential of iron oxide nanoparticles for combined tumor-targeting drug delivery as well as multimodality imaging.

4 Clinical Translation of PET Image-Guided Drug Delivery Using Nanoplatforms

Almost all the studies reported to date on PET image-guided drug delivery using nanoplatforms are limited to preclinical settings. Therefore, it must be admitted that this field is still in its nascent stage and more systematic studies are warranted to understand the mechanisms for targeting, drug delivery, and monitoring therapeutic efficacy, which might aid in translating these novel discoveries into real clinical impact. To successfully translate these theranostic nanoplatforms into the clinic, the following points need to be taken into consideration [54, 55].

- Several nanoplatforms are already used in patients for targeted drug delivery, as well as many are close to clinical translation [2, 3, 7]. Research efforts should be directed toward radiolabeling these nanoplatforms with suitable positron emitting radioisotopes to realize the scope PET image-guided drug delivery in near future. Given their established physicochemical versatility, and the large amount of preclinical studies already carried out, it can be expected that clinical translation of these radiolabeled nanomedicines will not be too problematic.
- Thorough knowledge needs to be gained regarding the pharmacokinetics and pharmacodynamics of the radiolabeled nanoplatforms loaded with chemotherapeutic drugs [54].
- It will be of paramount importance to establish that the degree of tumor accumulation of a radiolabeled nanoplatform loaded with drug as demonstrated by PET imaging should correspond, at least to some extent, to its therapeutic efficacy [54].
- Even if clear correlation between tumor accumulation of drug-loaded radiolabeled nanoplatform and its therapeutic efficacy is established, it will be essential to appropriately distinguish between low and high levels of target site accumulation. With the present knowledge, it is difficult to decide from what (relative) percentages of the injected dose onward, the patients can be expected to demonstrate adequately high levels of target site accumulation [54]. Obviously, these values will vary not only from one nanoplatform to the other but also from one type of malignancy to the other. Therefore, systematic and meticulously planned preclinical studies would be essential to provide answers to such questions.
- It would be important to understand how the level of target site accumulation of drug-loaded and radiolabeled nanoplatforms changes during the course of therapy [54]. In case the size, stage, perfusion, and/or permeability of tumors decrease significantly during the initial cycles of PET image-guided therapy, and if this also substantially lowers the degree of accumulation of the radiolabeled nanoplatform, then it will be essential to establish parameters and protocols to decide whether this treatment should be continued or not.

- Though not an essential criterion, it would be desirable to investigate how targeting and treating primary tumors with drug-loaded nanoplatfoms correlates with targeting and treatment of metastases.

Besides these biological aspects, there are several technical and regulatory issues that are also of paramount importance for clinical translation of the radiolabeled nanoplatfoms for PET image-guided drug delivery, as briefly enlisted later.

- As the theranostic nanoplatfoms are intended for human use, their preparation must adhere to current good manufacturing process (cGMP) compliance to ensure that the quality of the final product meet the acceptance criteria. The United States FDA has approved a set of regulations describing production of molecular imaging agents according to cGMP, outlined in the Code of Federal Regulations [15, 56–59]. Enforcement of cGMP is intended to preclude patients at risk due to inadequate safety and quality, and to enhance consistency in the application of the regulatory requirements [15, 56–59]. Any deviation from the approved method of preparation would require considerable validation before patient use.
- While ensuring cGMP compliance is an appealing vision, it is a demanding task as it includes requirement of well-qualified personnel, use of controlled materials and procedures, accessibility of qualified equipment, preparation of radiolabeled and drug-loaded nanoplatfoms in designated clean areas, applying only validated processes and analytical methods for each step, full documentation of the process, registration of the theranostic agent and clinical procedure to be adopted for PET image-guided drug delivery with national/regional health authorities, and release of the same for human use by an authorized personnel.
- While manual synthesis approach is generally adopted for synthesis of theranostics nanoplatfoms for PET image-guided drug delivery in a preclinical setting due to the requirement of the theranostic agents in small quantities, use of manual synthesis procedure for large-scale clinical applications might be challenging. Therefore, it might be essential to consider the use of automated synthesis apparatus owing to the following advantages [60, 61]:
 - Offer robust, repeatable synthesis of the theranostic nanoplatfoms.
 - Reduced operator intervention minimizes operational errors.
 - Ensure radiation safety during the radiolabeling step through reduction or elimination of manual operations.
- The use of fully automated synthesis modules not only facilitates cGMP compliance, but also offers complete traceability of the process, an aspect of utmost importance because of the extensive regulatory burden.
- Precludes the risk of bacterial contamination of the drug-loaded and radiolabeled nanoplatfoms that will be administered in human subjects.

Although automation strategy holds significant promise toward clinical translation of theranostics nanoplatfoms, it is associated with the challenge of reconfiguring the synthesis module for new procedures requiring nonconventional chemistry while maintaining full automation and compliance with cGMP regulations. Nevertheless, in order to be effective in addressing the particular regulatory barriers, automated synthesis modules must be customized to local legislative, regulatory, and institutional conditions.

It is also pertinent to point out that besides scientific and technical issues, several socioeconomic and political factors might also affect clinical translation of theranostic nanoplatfoms for PET image-guided drug delivery. The acceptance of a new approach in cancer management is generally an iterative process that requires substantial effort and sometimes luck. Extensive regulatory requirements and bureaucratic procedures in certain countries, limited potential market initially for such novel approaches, lobbying by the manufacturers of other approved cancer drugs, lack of reimbursement strategies by the insurance companies for these novel approaches, etc. might also impede the process of clinical translation of theranostic nanoplatfoms for PET image-guided drug delivery. Despite these hurdles, the exciting results obtained to date indicate that theranostic nanoplatfoms likely will have multifaceted applications in future clinical practice.

5 Conclusions and Future Perspectives

The versatility of theranostic nanoplatfoms for PET image-guided drug delivery brings forth unique perspectives in cancer management that are evident in their discovery and rapid development. A single nanoplatfom can now be used to detect tumors, treat them, monitor treatment response, and also guide therapeutic regimes. If the growth of this field continues at its present pace, the day may not be far out when PET image-guided drug delivery would become the norm rather than the exception in clinical oncology. However, before this optimism becomes a reality, several issues related to safety and complexity of theranostic nanoplatfoms must be adequately addressed. Generally, vascular-targeted delivery is only achievable using theranostic nanoplatfoms and penetration of cancerous drugs inside cancerous lesions has not yet fully succeeded [27]. Furthermore, cellular toxicity of several nanoplatfoms proposed for cancer theranostics is an issue of serious concern [27]. In general, biocompatible and biodegradable nanomaterials would be the preferred choice for clinical use in PET image-guided drug delivery.

Despite excellent attributes of PET, there is now an overwhelming scientific consensus that no single molecular imaging modality is perfect and sufficient to gain all the necessary information [17]. The multifunctionality of the nanoplatfoms would offer the scope for multimodality molecular imaging to provide synergistic advantages over any single modality alone. Similarly, it might be worth investigating the advantages of multimodality therapy wherein different types of therapeutic agents (such as chemotherapy, radiotherapy, or gene therapy agents) can be simultaneously delivered by the nanoplatfoms at cancerous lesions for enhanced therapeutic effectiveness. While numerous challenges face all new technologies, bringing theranostic nanoplatfoms for PET image-guided drug delivery to clinical market would require multidisciplinary effort at the intersection of manufacturing, regulation, and funding in order to turn these challenges into opportunities. Such a concerted effort may contribute toward developing more effective and less toxic treatment regimens for individual patients which would be a significant advancement toward achieving the ultimate goal of “personalized medicine” for cancer management.

Acknowledgments This work is supported, in part, by the University of Wisconsin—Madison, the Bhabha Atomic Research Centre (XII-N-R&D-004.01), the National Institutes of Health (NIBIB/NCI 1R01CA169365, P30CA014520, and 5T32GM08349), the Department of Defense (W81XWH-11-1-0644), the American Cancer Society (125246-RSG-13-099-01-CCE), and the National Science Foundation (DGE-1256259).

References

1. Bregoli L, Movia D, Gavigan-Imedio JD, Lysaght J, Reynolds J, Prina-Mello A. Nanomedicine applied to translational oncology: a future perspective on cancer treatment. *Nanomedicine*. 2016;12:81–103.
2. Lytton-Jean AK, Kauffman KJ, Kaczmarek JC, Langer R. Cancer nanotherapeutics in clinical trials. *Cancer Treat Res*. 2015;166:293–322.
3. Perez-Herrero E, Fernandez-Medarde A. Advanced targeted therapies in cancer: drug nanocarriers, the future of chemotherapy. *Eur J Pharm Biopharm*. 2015;93:52–79.
4. Jemal A, Center MM, DeSantis C, Ward EM. Global patterns of cancer incidence and mortality rates and trends. *Cancer Epidemiol Biomarkers Prev*. 2010;19(8):1893–907.
5. World Health Organization Cancer Factsheet. (<http://www.who.int/mediacentre/factsheets/fs297/en/>). Accessed 20 Sept 2015.
6. Zhang Y, Chan HF, Leong KW. Advanced materials and processing for drug delivery: the past and the future. *Adv Drug Deliv Rev*. 2013;65(1):104–20.
7. Marchal S, Hor AE, Millard M, Gillon V, Bezdetnaya L. Anticancer drug delivery: an update on clinically applied nanotherapeutics. *Drugs*. 2015;75:1601–11.
8. Terreno E, Uggeri F, Aime S. Image guided therapy: the advent of theranostic agents. *J Control Release*. 2012;161(2):328–37.
9. Chow EK, Ho D. Cancer nanomedicine: from drug delivery to imaging. *Sci Transl Med*. 2013;5(216):216rv4.
10. Chen F, Ehlerding EB, Cai W. Theranostic nanoparticles. *J Nucl Med*. 2014;55(12):1919–22.
11. Chakravarty R, Hong H, Cai W. Positron emission tomography image-guided drug delivery: current status and future perspectives. *Mol Pharm*. 2014;11(11):3777–97.
12. Chakravarty R, Hong H, Cai W. Image-guided drug delivery with single-photon emission computed tomography: a review of literature. *Curr Drug Targets*. 2015;16(6):592–609.
13. Jokerst JV, Gambhir SS. Molecular imaging with theranostic nanoparticles. *Acc Chem Res*. 2011;44(10):1050–60.
14. Pancholi K. A review of imaging methods for measuring drug release at nanometre scale: a case for drug delivery systems. *Expert Opin Drug Deliv*. 2012;9(2):203–18.
15. Chakravarty R, Chakraborty S, Dash A. Molecular imaging of breast cancer: role of RGD peptides. *Mini Rev Med Chem*. 2015.
16. Ametamey SM, Honer M, Schubiger PA. Molecular imaging with PET. *Chem Rev*. 2008;108(5):1501–16.
17. Jennings LE, Long NJ. “Two is better than one”—probes for dual-modality molecular imaging. *Chem Commun (Camb)*. 2009;(24):3511–24.
18. Aboagye EO, Price PM. Use of positron emission tomography in anticancer drug development. *Invest New Drugs*. 2003;21(2):169–81.
19. Alauddin MM. Positron emission tomography (PET) imaging with ^{18}F -based radiotracers. *Am J Nucl Med Mol Imaging*. 2012;2(1):55–76.
20. Rosch F. Past, present and future of $^{68}\text{Ge}/^{68}\text{Ga}$ generators. *Appl Radiat Isot*. 2013;76:24–30.
21. Chakravarty R, Valdovinos HF, Chen F, Lewis CM, Ellison PA, Luo H, et al. Intrinsically germanium-69-labeled iron oxide nanoparticles: synthesis and in-vivo dual-modality PET/MR imaging. *Adv Mater*. 2014;26(30):5119–23.
22. Chen F, Ellison PA, Lewis CM, Hong H, Zhang Y, Shi S, et al. Chelator-free synthesis of a dual-modality PET/MRI agent. *Angew Chem Int Ed Engl*. 2013;52(50):13319–23.

23. Chen F, Goel S, Valdovinos HF, Luo H, Hernandez R, Barnhart TE, et al. In vivo integrity and biological fate of chelator-free zirconium-89-labeled mesoporous silica nanoparticles. *ACS Nano*. 2015;9(8):7950–9.
24. Pagani M, Stone-Elander S, Larsson SA. Alternative positron emission tomography with non-conventional positron emitters: effects of their physical properties on image quality and potential clinical applications. *Eur J Nucl Med*. 1997;24(10):1301–27.
25. Kornyei J, Mikecz P, Toth G. PET radiopharmaceuticals: novelties and new possibilities. *Magy Onkol*. 2014;58(4):245–50.
26. Zhang R, Fan Q, Yang M, Cheng K, Lu X, Zhang L, et al. Engineering melanin nanoparticles as an efficient drug-delivery system for imaging-guided chemotherapy. *Adv Mater*. 2015;27(34):5063–9.
27. Lanza GM, Moonen C, Baker Jr JR, Chang E, Cheng Z, Grodzinski P, et al. Assessing the barriers to image-guided drug delivery. *Wiley Interdiscip Rev Nanomed Nanobiotechnol*. 2014;6(1):1–14.
28. Kunjachan S, Pola R, Gremse F, Theek B, Ehling J, Moeckel D, et al. Passive versus active tumor targeting using RGD- and NGR-modified polymeric nanomedicines. *Nano Lett*. 2014;14(2):972–81.
29. Ernsting MJ, Murakami M, Roy A, Li SD. Factors controlling the pharmacokinetics, biodistribution and intratumoral penetration of nanoparticles. *J Control Release*. 2013;172(3):782–94.
30. van Vlerken LE, Vyas TK, Amiji MM. Poly(ethylene glycol)-modified nanocarriers for tumor-targeted and intracellular delivery. *Pharm Res*. 2007;24(8):1405–14.
31. Goyal P, Goyal K, Vijaya Kumar SG, Singh A, Katare OP, Mishra DN. Liposomal drug delivery systems—clinical applications. *Acta Pharm*. 2005;55(1):1–25.
32. Medina OP, Zhu Y, Kairemo K. Targeted liposomal drug delivery in cancer. *Curr Pharm Des*. 2004;10(24):2981–9.
33. Paoli EE, Kruse DE, Seo JW, Zhang H, Kheiriloomoom A, Watson KD, et al. An optical and microPET assessment of thermally-sensitive liposome biodistribution in the Met-1 tumor model: importance of formulation. *J Control Release*. 2010;143(1):13–22.
34. Lee H, Zheng J, Gaddy D, Orcutt KD, Leonard S, Geretti E, et al. A gradient-loadable ⁶⁴Cu-chelator for quantifying tumor deposition kinetics of nanoliposomal therapeutics by positron emission tomography. *Nanomedicine*. 2015;11(1):155–65.
35. Kedar U, Phutane P, Shidhaye S, Kadam V. Advances in polymeric micelles for drug delivery and tumor targeting. *Nanomedicine*. 2010;6(6):714–29.
36. Gothwal A, Khan I, Gupta U. Polymeric micelles: recent advancements in the delivery of anticancer drugs. *Pharm Res*. 2016;33:18–39.
37. Xiao Y, Hong H, Javadi A, Engle JW, Xu W, Yang Y, et al. Multifunctional unimolecular micelles for cancer-targeted drug delivery and positron emission tomography imaging. *Biomaterials*. 2012;33(11):3071–82.
38. Guo J, Hong H, Chen G, Shi S, Zheng Q, Zhang Y, et al. Image-guided and tumor-targeted drug delivery with radiolabeled unimolecular micelles. *Biomaterials*. 2013;34(33):8323–32.
39. Guo J, Hong H, Chen G, Shi S, Nayak TR, Theuer CP, et al. Theranostic unimolecular micelles based on brush-shaped amphiphilic block copolymers for tumor-targeted drug delivery and positron emission tomography imaging. *ACS Appl Mater Interfaces*. 2014;6(24):21769–79.
40. Huard DJ, Kane KM, Tezcan FA. Re-engineering protein interfaces yields copper-inducible ferritin cage assembly. *Nat Chem Biol*. 2013;9(3):169–76.
41. Ren G, Miao Z, Liu H, Jiang L, Limpa-Amara N, Mahmood A, et al. Melanin-targeted preclinical PET imaging of melanoma metastasis. *J Nucl Med*. 2009;50(10):1692–9.
42. Webb JA, Bardhan R. Emerging advances in nanomedicine with engineered gold nanostructures. *Nanoscale*. 2014;6(5):2502–30.
43. Mody VV, Siwale R, Singh A, Mody HR. Introduction to metallic nanoparticles. *J Pharm Bioallied Sci*. 2010;2(4):282–9.
44. Xiao Y, Hong H, Matson VZ, Javadi A, Xu W, Yang Y, et al. Gold nanorods conjugated with doxorubicin and cRGD for combined anticancer drug delivery and PET imaging. *Theranostics*. 2012;2(8):757–68.

45. Shi S, Chen F, Cai W. Biomedical applications of functionalized hollow mesoporous silica nanoparticles: focusing on molecular imaging. *Nanomedicine*. 2013;8(12):2027–39.
46. El-Hammadi MM, Arias JL. Iron oxide-based multifunctional nanoparticulate systems for biomedical applications: a patent review (2008—present). *Expert Opin Ther Pat*. 2015;25(6):691–709.
47. Sharifi S, Seyednejad H, Laurent S, Atyabi F, Saei AA, Mahmoudi M. Superparamagnetic iron oxide nanoparticles for in vivo molecular and cellular imaging. *Contrast Media Mol Imaging*. 2015.
48. US FDA Investigational New Drug approval for first-in-human trial of novel cancer-targeting nanoparticle. *News Anal Ther Deliv*. 2011;2(3):287.
49. Chen F, Hong H, Zhang Y, Valdovinos HF, Shi S, Kwon GS, et al. In vivo tumor targeting and image-guided drug delivery with antibody-conjugated, radiolabeled mesoporous silica nanoparticles. *ACS Nano*. 2013;7(10):9027–39.
50. Goel S, Chen F, Hong H, Valdovinos HF, Hernandez R, Shi S, et al. VEGF₁₂₁-conjugated mesoporous silica nanoparticle: a tumor targeted drug delivery system. *ACS Appl Mater Interfaces*. 2014;6(23):21677–85.
51. Chen F, Hong H, Shi S, Goel S, Valdovinos HF, Hernandez R, et al. Engineering of hollow mesoporous silica nanoparticles for remarkably enhanced tumor active targeting efficacy. *Sci Rep*. 2014;4:5080.
52. Chakravarty R, Goel S, Hong H, Chen F, Valdovinos HF, Hernandez R, et al. Hollow mesoporous silica nanoparticles for tumor vasculature targeting and PET image-guided drug delivery. *Nanomedicine*. 2015;10(8):1233–46.
53. Yang X, Hong H, Grailer JJ, Rowland IJ, Javadi A, Hurley SA, et al. cRGD-functionalized, DOX-conjugated, and ⁶⁴Cu-labeled superparamagnetic iron oxide nanoparticles for targeted anticancer drug delivery and PET/MR imaging. *Biomaterials*. 2011;32(17):4151–60.
54. Lammers T, Rizzo LY, Storm G, Kiessling F. Personalized nanomedicine. *Clin Cancer Res*. 2012;18(18):4889–94.
55. Theek B, Rizzo LY, Ehling J, Kiessling F, Lammers T. The theranostic path to personalized nanomedicine. *Clin Transl Imaging*. 2014;2(1):66–76.
56. Regulations for in vivo radiopharmaceuticals used for diagnosis and monitoring. Food and Drug Administration, HHS. Final rule. *Fed Regist*. 1999;64(94):26657–70.
57. Harold J. What is now current good manufacturing practice for PET drugs? *Clin Nucl Med*. 2010;35(5):329.
58. Hung JC. USP general chapter <797> pharmaceutical compounding-sterile preparations. *J Nucl Med*. 2004;45(6):20N. 8N.
59. Hung JC. The potential impact of usp general chapter <797> on procedures and requirements for the preparation of sterile radiopharmaceuticals. *J Nucl Med*. 2004;45(6):21N–6.
60. Boschi S, Malizia C, Lodi F. Overview and perspectives on automation strategies in ⁶⁸Ga radiopharmaceutical preparations. *Recent Results Cancer Res*. 2013;194:17–31.
61. Chi YT, Chu PC, Chao HY, Shieh WC, Chen CC. Design of CGMP production of ¹⁸F- and ⁶⁸Ga-radiopharmaceuticals. *Biomed Res Int*. 2014;2014:680195.